JOURNAL OF VIROLOGY, Feb. 2009, p. 1320–1331 Vol. 83, No. 3
0022-538X/09/$08.00+0 doi:10.1128/JVI.00977-08

Avian Influenza A Virus Polymerase Association with Nucleoprotein, but Not Polymerase Assembly, Is Impaired in Human Cells during the Course of Infection▽

Marie-Anne Rameix-Welti, Andru Tomoiu, Emmanuel Dos Santos Afonso, Sylvie van der Werf, and Nadia Naffakh*

Institut Pasteur, Unité de Génétique Moléculaire des Virus Respiratoires, URA CNRS 3015, EA302 Université Paris Diderot, Paris, France

Received 10 May 2008/Accepted 13 November 2008

Strong determinants of the host range of influenza A viruses have been identified on the polymerase complex formed by the PB1, PB2, and PA subunits and on the nucleoprotein (NP). In the present study, molecular mechanisms that may involve these four core proteins and contribute to the restriction of avian influenza virus multiplication in human cells have been investigated. The efficiencies with which the polymerase complexes of a human and an avian influenza virus isolate assemble and interact with the viral NP and cellular RNA polymerase II proteins were compared in mammalian and in avian infected cells. To this end, recombinant influenza viruses expressing either human or avian-derived core proteins with a PB2 protein fused to the One-Strep purification tag at the N or C terminus were generated. Copurification experiments performed on infected cell extracts indicate that the avian-derived polymerase is assembled and interacts physically with the cellular RNA polymerase II at least as efficiently as does the human-derived polymerase in human as well as in avian cells. Restricted growth of the avian isolate in human cells correlates with low levels of the core proteins in infected cell extracts and with poor association of the NP with the polymerase compared to what is observed for the human isolate. The NP-polymerase association is restored by a Glu-to-Lys substitution at residue 627 of PB2. Overall, our data point to viral and cellular factors regulating the NP-polymerase interaction as key determinants of influenza A virus host range. Recombinant viruses expressing a tagged polymerase should prove useful for further studies of the molecular interactions between viral polymerase and host factors during the infection cycle.

Avian influenza viruses usually do not replicate or cause disease in humans, but they have the potential to adapt to humans and initiate a pandemic (29, 38). The molecular determinants and related mechanisms that may restrict or favor the multiplication of avian influenza viruses in humans remain poorly understood. Some determinants of host range are related to the receptor specificity of the surface glycoproteins (30, 34). Genetic analyses also hint at a major role of the viral ribonucleoproteins (RNPs) in host range (for a review, see references 25 and 29). The RNPs are formed of the viral RNAs (vRNAs) associated with the nucleoprotein (NP) and the heterotrimeric PB1-PB2-PA polymerase (Pol) complex. Experimental adaptation of an avian (10) or an equine (33) virus to mice was shown to be driven mainly by mutations on the genes encoding the viral Pol and NP, which correspond to the minimum set of proteins required for both the transcription and replication of vRNAs. A correlation between the levels of activity of the viral Pol in mammalian cultured cells and the replication potential in mammalian hosts has been observed (9, 16, 31). An increased replication rate probably determines the ability of the virus to outcompete the innate and immune responses and to establish a successful infection. It might also increase the chances for variants with a higher fitness in the new host to be generated and selected.

It is generally assumed that adaptative mutations on the RNPs lead to an optimized interaction with host factors. Once released in the cytoplasm of the infected cell, the RNPs are transported to the nucleus, where transcription and replication of the vRNAs take place in close association with the cellular transcriptional machinery. Viral transcription is particularly dependent on the host RNA PolII activities (for a review, see references 6 and 28). Newly formed vRNAs, packaged as RNPs, may serve as templates for secondary rounds of transcription/replication or may exit the nucleus to be incorporated into progeny virions. Upon transmission to a new species, the assembly, transport, stability, and/or activity of the viral RNPs could be altered due to inefficient or inappropriate association with cellular factor(s). The existence of a physical association between the PB1-PB2-PA heterotrimer and the cellular RNA Pol II has been recently described (7). Other cellular proteins involved in cellular RNA synthesis, modification, and translation (13, 14, 24, 26) and also proteins involved in cellular DNA replication (15, 22) and in nucleo-cytoplasmic trafficking (2, 5, 35), as well as members of the chaperone (12, 27) and cytoskeleton (3) family of proteins, have been found to interact with influenza virus RNP components. However, little is known about the importance of such molecular interactions with respect to host adaptation.

In the present study, we show that recombinant influenza viruses expressing a PB2 protein fused to the One-Strep puri-

* Corresponding author. Mailing address: Unité de Génétique Moléculaire des Virus Respiratoires, URA CNRS 3015, Institut Pasteur, 25 rue du Dr. Roux, 75724 Paris Cedex 15, France. Phone: 33 1 45 68 88 11. Fax: 33 1 40 61 32 41. E-mail: nnaffakh@pasteur.fr.

▽ Published ahead of print on 19 November 2008.

fication tag are an appropriate tool to investigate molecular interactions involving viral RNPs in the context of an infectious cycle. By using this strategy, the efficiency with which the RNP components of a human and an avian influenza virus isolate interact with each other and with the cellular RNA Pol II was compared in mammalian and in avian infected cells. Our results indicate that the Pol complex of an avian influenza virus gets assembled upon infection of a human cell and interacts physically with the human RNA Pol II enzyme at least as efficiently as does the Pol complex of a human influenza virus. However, the restricted growth of the avian influenza virus in human cells correlates with a poor association of the NP with the Pol complex.

MATERIALS AND METHODS

Cell and viruses. 293T and DF1 cells were grown in complete Dulbecco's modified Eagle's medium (DMEM) supplemented with 10% fetal calf serum (FCS). QT6 cells were grown in Ham-F10 medium supplemented with 10% FCS, 1% chicken serum, and 2% tryptose phosphate broth. MDCK cells were grown in modified Eagle's medium supplemented with 5% FCS.

Influenza viruses A/Paris/908/97 ([P908] H3N2) and A/Mallard/Marquenterre/Z237/83 ([MZ] H1N1) were isolated by the National Influenza Center (northern France) at the Pasteur Institute in Paris (France). Viruses P908 and MZ were propagated in MDCK cells and embryonated hen eggs, respectively.

Plaque assays. Unless indicated otherwise, P908- and MZ-derived viruses were titrated on MDCK and QT6 cells, respectively, using a plaque assay procedure adapted from Matrosovich et al. (21). When MDCK cells were used, the overlay was prepared with 1.2% Avicel (RC581; FMC BioPolymer) in complete minimal essential medium (MEM) and L-(tosylamido-2-phenyl) ethyl chloromethyl ketone (TPCK)-trypsin (Worthington) at a final concentration of 1 μg/ml. When QT6 cells were used, the overlay was prepared with 0.3% Avicel, 25% MEM, 75% Ham-10 medium, and TPCK-trypsin at a final concentration of 0.25 to 0.4 μg/ml.

Plasmids. The four plasmids containing the promoter of Pol I (pPol I) encoding the sequences corresponding to the hemagglutinin (HA), neuraminidase, M, and NS genomic segments of A/WSN/33 (WSN) virus (8) were kindly provided by G. Brownlee (Sir William Dunn School of Pathology, Oxford, United Kingdom). Plasmids pHMG-PB1, -PB2, -PA, and -NP, encoding the PB1, PB2, PA, and NP proteins of influenza viruses P908 and MZ have been described earlier (16). The PB1, PB2, PA, and NP cDNAs were amplified using the recombinant pHMG plasmids as templates and primers specific for the coding sequences that contained additional nucleotides corresponding to the 3′ noncoding region (NCR) and 5′ NCR of the PB1, PB2, PA, and NP genomic segments, respectively, of the WSN virus. The amplicons were cloned between the two BbsI sites of the pPR7 plasmid (1), resulting in pPR7-P908-PB1, pPR7-P908-PB2, pPR7-P908-PA, and pPR7-P908-NP plasmids on the one hand, and pPR7-MZ-PB1, pPR7-MZ-PB2, pPR7-MZ-PA, and pPR7-MZ-NP plasmids on the other hand. The following sequences were fused to the last amino acid of the PB2 open reading frame (ORF) into the pPR7-P908-PB2 and pPR7-MZ-PB2 plasmids using standard PCR and cloning procedures: (i) a linker sequence encoding three Ala residues, (ii) the HA tag (YPYDVPDYA) or the One-Strep tag (WSHPQFEKGGGSGGGSGGGSWSHPQFEK) coding sequence, (iii) a stop codon combined with an NheI restriction site (TAGCATGC), and (iv) the 5′ terminal 143 nucleotides of the PB2 segment. Alternatively, the One-Strep tag sequence followed by a linker sequence encoding three Ala residues was inserted upstream of the PB2 ORF into the pPR7-P908-PB2 and pPR7-MZ-PB2 plasmids. The E627K mutation was introduced in the pPR7-MZ-PB2 plasmids by site-directed mutagenesis using a QuickChange Site-Directed Mutagenesis kit (Stratagene). All constructs were verified by sequencing positive clones using a Big Dye terminator sequencing kit and an automated sequencer (Perkin Elmer). The sequences of the oligonucleotides used for amplification and sequencing can be provided upon request.

Production of recombinant viruses by reverse genetics. The method used for the production of recombinant influenza viruses by reverse genetics was adapted from previously described procedures (8). Briefly, the four pPol I WSN plasmids, together with the four pPR7-P908 or pPR7-MZ plasmids (including pPR7-PB2, pPR7-PB2-HA, pPR7-PB2-Nstrep [where Nstrep indicates the presence of the One-Strep tag sequence at the N terminus], or pPR7-PB2-Cstrep [carrying the One-Strep tag at the C terminus]) and the corresponding four pHMG-P908 or pHMG-MZ plasmids (0.5 μg of each), were cotransfected into a subconfluent monolayer of cocultivated 293T and MDCK cells (4×10^5 and 3×10^5 cells, respectively, seeded in a 35-mm dish), using 10 μl of the Fugene 6 transfection reagent (Roche). After 24 h of incubation at 37°C, the supernatant was removed, and cells were washed twice with DMEM and incubated at 37°C in DMEM containing TPCK-trypsin at a final concentration of 0.5 μg/ml for 48 h. The efficiency of reverse genetics was evaluated by titrating the supernatant on MDCK and QT6 cells in plaque assays.

Subsequent amplifications of the P908-WSN recombinant virus and derivatives were performed on MDCK cells at a multiplicity of infection (MOI) of 0.001 or 0.0001 for 2 to 3 days at 35°C in MEM containing TPCK-trypsin at a concentration of 1 μg/ml. The MZ-WSN recombinant virus and derivatives were amplified on DF1 cells at an MOI of 0.001 or 0.0001 for 2 to 3 days at 37°C in DMEM supplemented with 2.5% FCS. The exact conditions of amplification used for a given virus can be provided upon request.

vRNA extraction, RT-PCR, and sequence analysis. Viral RNA was prepared from all viral stocks using a QIAamp Viral RNA Mini kit (Qiagen) according to the manufacturer's recommendations. Five microliters of vRNA was subjected to reverse transcription PCR (RT-PCR) and amplification using a Titan One-Step RT-PCR kit (Roche). The PB1, PB2, PA, and NP segments of the P908-WSN and MZ-WSN viruses and the PB2 segments of the tagged viruses and of a PB2 mutant virus carrying a Glu-to-Lys substitution at residue 627 (PB2-627) were amplified as one single amplicon, using specific oligonucleotides anchored on the 3′ and 5′ terminal 22 to 38 nucleotides of the segment, or as two overlapping amplicons, in which case an additional pair of internal oligonucleotides was used. The products of amplification were purified using a QIAquick gel extraction kit (Qiagen) and sequenced using a Big Dye terminator sequencing kit and an automated sequencer (Perkin Elmer). The sequences of the oligonucleotides used for amplification and sequencing can be provided upon request.

Purification of the PB2 proteins fused to the One-Strep tag (PB2-Strep) on Strep-tactin beads. At 6 h following infection of 293T cells (2×10^7 cells in 100-mm dishes) or DF1 cells (5×10^6 cells in 100-mm dishes) with the PB2-wild type (wt) and PB2-Cstrep or PB2-wt and PB2-Nstrep viruses at an MOI of 2, cells were washed twice with phosphate-buffered saline (PBS), collected with a cell scraper, and centrifuged at $450 \times g$ for 5 min. The packed cell volume was estimated. Cells were resuspended in five packed cell volumes of a lysis buffer containing 50 mM Tris-HCl, pH 8, 300 mM NaCl, 2 mM $MgCl_2$, 0.3% NP-40, 1 mM dithiothreitol, 10% glycerol, 1× protease inhibitor cocktail (Sigma), and 0.25 μ/ml of benzonase nuclease (Novagen). Cell lysates were incubated on a wheel for 1 h at 4°C and then centrifuged at $16{,}000 \times g$ for 20 min. The supernatant was transferred to a fresh tube, 1/20 of the volume was frozen at −80°C, and the remaining volume was incubated on a wheel overnight with 1 mg of Strep-tactin beads (IBA GmbH). The beads were washed as recommended by the supplier, and bound proteins were eluted in 50 μl of Laemmli buffer, preheated at 95°C for most experiments, or in 50 μl of elution buffer containing 2.5 mM desthiobiotin (IBA GmbH) when the Nstrep viruses were used.

Western blot assays. Cell lysates and Strep-tactin elution samples were analyzed by electrophoresis on a denaturing NuPAGE 4 to 12% Bis-Tris gel (Invitrogen), followed by Western blotting using polyvinylidene difluoride membranes. The membranes were incubated overnight at 4°C with a mouse monoclonal antibody directed against the C-terminal domain of RNA Pol II (diluted 1:1,000; 8WG16; Covance) or with rabbit polyclonal antibodies directed against the PB1, PB2, or PA proteins (diluted 1:5,000; kindly provided by J. Ortin, Centro Nacional de Biotecnologia, Madrid, Spain) or against A/PR/8/34 virions (37) (diluted 1:10,000 for the detection of NP and M1 proteins) in PBS with 1% bovine serum albumin, and 0.25% Tween 20. Membranes were then incubated for 1 h at room temperature with peroxidase-conjugated secondary antibodies (GE Healthcare), and with the ECL+ substrate (GE Healthcare). After the membranes were scanned using a G-Box (SynGene), the signals corresponding to the PB2, PB1, PA, NP, or RNA Pol II proteins were quantified using the GeneTools software (SynGene).

Indirect immunofluorescence assay. Semiconfluent 293T cells on coverslips were infected with the PB2-wt or PB2-HA recombinant viruses at an MOI of 2. At 2 and 6 h postinfection (p.i.), cells were fixed with PBS–4% paraformaldehyde for 20 min, permeabilized with PBS–0.1% Triton X-100 for 10 min, and then incubated with either the 16B12 anti-HA (Covance) or IA-52 anti-NP (Oxford Biotechnology) monoclonal antibody, diluted 1:200. After subsequent incubation with AlexaFluor 555-coupled anti-mouse immunoglobulin G and AlexaFluor 488-coupled anti-rabbit immunoglobulin G secondary antibodies (diluted 1:500; Molecular Probes), the samples were analyzed under a fluorescence microscope (Leica).

RESULTS

Production of reassortant influenza viruses with core proteins derived from an avian or a human influenza virus isolate. Recombinant viruses expressing the core proteins (PB1, PB2, PA, and NP) derived from the human isolate P908 or from the avian isolate MZ in a WSN virus background were produced by reverse genetics, as described in the Materials and Methods section. The resulting P908-WSN and MZ-WSN viruses were amplified on MDCK (mammalian: canine) and DF1 (avian: chicken) cells, respectively. vRNA was extracted and subjected to RT-PCR using primers designed to amplify the whole PB1, PB2, PA, and NP segments. Direct sequencing of the PCR products demonstrated that the PB1, PB2, PA, and NP coding sequences were unchanged in the P908-WSN and MZ-WSN reassortant viruses compared to the P908 and MZ parental viruses, respectively (data not shown).

MDCK cells were infected at an MOI of 0.001 and incubated at 37, 35, or 33°C for 72 h. Virus titers in the culture supernatant were determined at different times p.i. by plaque assays. Viral multiplication was only moderately affected by temperature variations for P908 and P908-WSN viruses (Fig. 1A), whereas it was strongly delayed at low temperatures in the case of MZ and MZ-WSN (Fig. 1B), in agreement with our previous observations (16, 20). The growth curves of P908 and P908-WSN viruses were very similar: maximum titers were observed at 48 h p.i. with a 2-fold (at 37°C) to 13-fold (at 33°C) difference in favor of P908 (Fig. 1A). In contrast, at 48 h p.i., the MZ virus grew to titers 5-fold (at 37°C) to 10-fold (at 33°C) lower than those of the reassortant MZ-WSN virus (Fig. 1B). As a consequence, the growth advantage of P908 over MZ was attenuated when P908-WSN and MZ-WSN were compared (e.g., at 48 h p.i. the difference in titers between the reassortant viruses compared to the difference between the parental viruses was about 1 log versus 2 log at 37°C, 2 log versus 4 log at 35°C, and 4 log versus 6 log at 33°C). Still, the P908-WSN virus conserved a clear growth advantage over MZ-WSN.

Host range and temperature sensitivity of the parental and reassortant viruses were further examined by performing plaque assays at 37 or 33°C on MDCK and QT6 (avian: quail) cells in parallel. Plaques formed by the avian-derived MZ and MZ-WSN viruses were reduced in number and in size on MDCK (Fig. 1D) compared to QT6 cells (Fig. 1F). Sensitivity to low temperatures of these viruses was very apparent on MDCK cells, as almost no visible plaques were formed at 33°C even when lower dilutions of the viral stock were tested (Fig. 1D). This was not the case on QT6 cells, where plaque size was only slightly reduced at 33 compared to 37°C (Fig. 1F). Unlike what was observed with MZ and MZ-WSN viruses, plaque formation by the human-derived P908 and P908-WSN viruses was more efficient on MDCK (Fig. 1C) than on QT6 cells (Fig. 1E). On MDCK cells, sensitivity to low temperatures of the P908 and P908-WSN viruses was very moderate compared to their MZ counterparts (compare Fig. 1C and D) although slightly more pronounced for the P908-WSN than for the P908 virus (Fig. 1C). On QT6 cells, sensitivity to low temperatures of the P908 and P908-WSN viruses was also moderate (Fig. 1E), as observed for the MZ and MZ-WSN viruses (Fig. 1F).

Overall, the P908-WSN and MZ-WSN reassortant viruses showed growth properties close to the parental P908 and MZ viruses, respectively. This similarity pointed to the fact that the differences between P908 and MZ with respect to growth potential and temperature sensitivity on mammalian cells were determined mainly by the RNP genes and validated the use of the reassortant viruses as a tool to further investigate the molecular mechanisms involved.

Production of influenza viruses expressing a PB2 protein fused to the One-Strep purification tag. The PB2 segment was further engineered in order to generate P908-WSN and MZ-WSN viruses expressing a PB2 protein fused to the One-Strep affinity purification tag, a polypeptide which binds specifically to a derivative of streptavidin called Strep-tactin (32). The sequence encoding the One-Strep tag was fused to the sequence encoding either the C terminus (Fig. 2A) or the N terminus of PB2 (Fig. 2B). In the former case, a duplication of the last 109 nucleotides encoding PB2 was inserted between the stop codon of the PB2-Strep sequence and the 5′ NCR in order to ensure the conservation of a packaging signal overlapping the coding and noncoding regions at the 5′ end of the segment, as described earlier (4) (Fig. 2A). The resulting P908-Cstrep-WSN and P908-Nstrep-WSN viruses were amplified on MDCK cells. The MZ-Cstrep-WSN and MZ-Nstrep-WSN viruses were amplified on DF1 cells. vRNA was extracted and subjected to RT-PCR using primers designed to amplify the whole PB2 segment. Direct sequencing of the PCR products confirmed that the One-Strep coding sequence was present, as well as the PB2-ORF duplication in the case of Cstrep viruses (data not shown).

Growth properties of the viruses expressing a tagged PB2 or a wt PB2 protein were compared at 37°C. The P908-Cstrep-WSN and P908-WSN viruses showed the same kinetics of multiplication following infection of MDCK cells at a low MOI (0.001) (Fig. 2C). The MZ-Cstrep-WSN virus grew at a slower rate than MZ-WSN and achieved much lower titers on MDCK cells (Fig. 2C), whereas both viruses showed similar growth curves on QT6 cells (Fig. 2E). Thus, the presence of the One-Strep tag at the C terminus of PB2 did not alter the fitness of the virus per se but caused a growth defect specifically in mammalian cells. The growth defect of the MZ-Cstrep-WSN virus on MDCK cells was also observed at 40°C (data not shown). Unlike the MZ-Cstrep-WSN virus, the MZ-Nstrep-WSN virus showed a growth curve similar to that of the MZ-WSN virus on MDCK cells (Fig. 2D).

Expression levels of the PB2, PB1, NP, and M1 proteins were examined in MDCK and QT6 cells infected at a high MOI with the PB2-Cstrep or PB2-Nstrep viruses or with the PB2-wt viruses as a control. Total cell extracts were prepared at 6 h p.i and were analyzed by Western blotting. Both the PB2-Strep and PB2-wt proteins were revealed when an anti-PB2 polyclonal antibody was used, whereas a monoclonal antibody specific for the One-Strep tag reacted exclusively with the PB2-Strep proteins (Fig. 3). The overall levels of PB2, PB1, NP, and M1 proteins were reduced in cells infected with the MZ-WSN viruses compared to their P908-WSN counterparts. This reduction was more pronounced in MDCK (Fig. 3) than in QT6 infected cells (Fig. 3). The presence of a One-Strep tag at the C terminus of PB2 had little effect on the accumulation of viral proteins, except for a fourfold increase of NP accumulation in cells infected with the P908-Cstrep-WSN compared to the P908-WSN virus (Fig. 3; also data not shown for the esti-

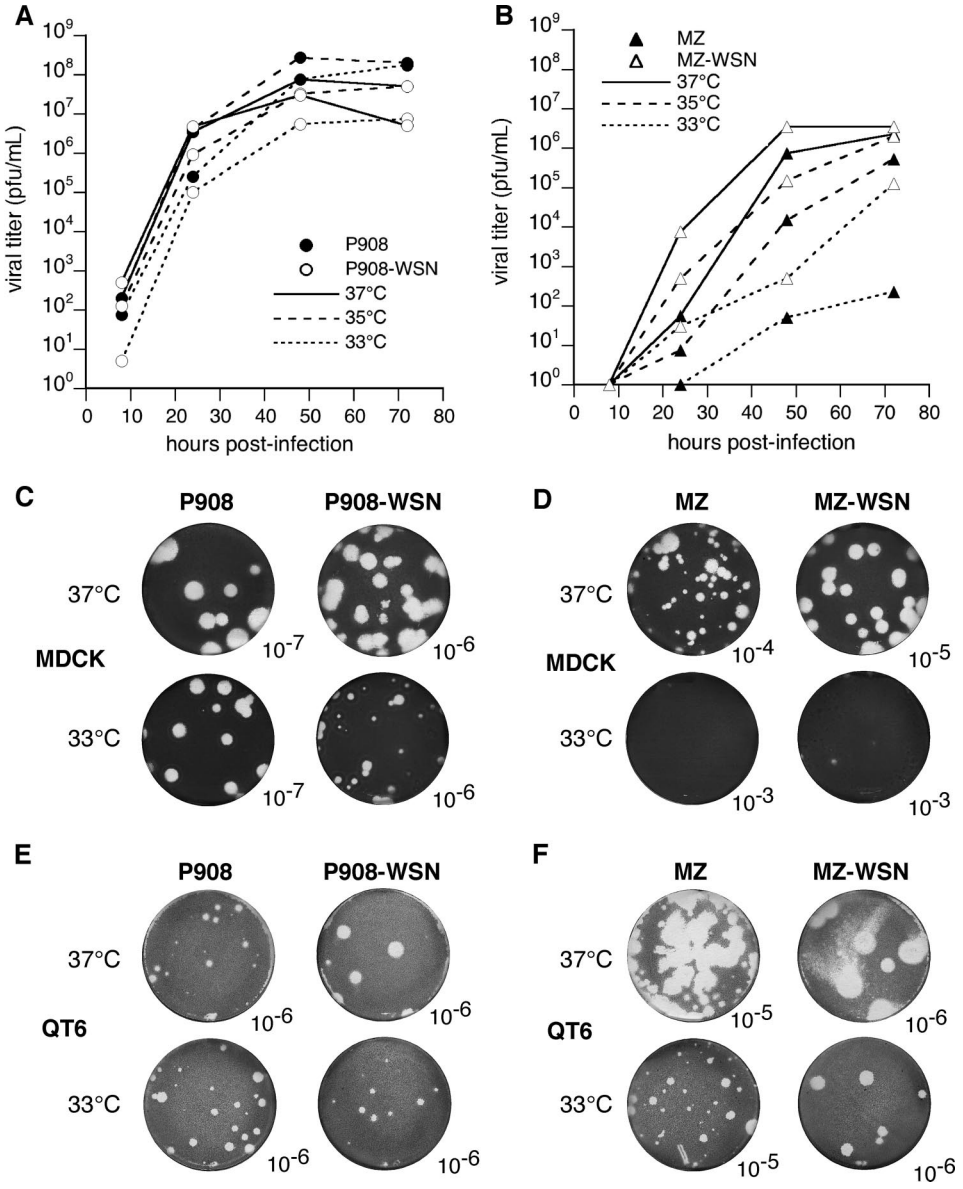

FIG. 1. Growth properties of recombinant influenza viruses expressing core proteins derived from the avian MZ or human P908 influenza virus isolate in the WSN background. (A) Growth curves of the parental P908 and reassortant P908-WSN viruses on MDCK cells. Cell monolayers were infected at an MOI of 0.001 and incubated for 72 h at 37, 35, or 33°C. At the indicated time points, the supernatants were harvested, and virus titers were determined by plaque assays on MDCK cells. (B) Growth curves of the parental MZ and reassortant MZ-WSN viruses on MDCK cells. Experimental conditions were as described in panel A, except that virus titers were determined on QT6 cells. (C to F) Plaque phenotype of the P908 and reassortant P908-WSN viruses (C and E) or MZ and reassortant MZ-WSN viruses (D and F) assayed on MDCK or QT6 cells, as described in Materials and Methods. Cell monolayers were stained with crystal violet after 72 h of incubation at 37 or 33°C. Representative data are shown. The dilutions of the viral stock used for infection are indicated.

mated fourfold difference based on Western blot analysis of serial dilutions of both types of cell extracts). Remarkably, the PB2, PB1, NP, and M1 proteins were detected at similar levels in MDCK cells infected with the MZ-Cstrep-WSN and MZ-WSN viruses (Fig. 3) (M1 signals were detectable only after a longer exposure time [data not shown]). This observation suggests that the reduced growth of the MZ-Cstrep-WSN virus observed upon multicycle multiplication on MDCK cells (Fig. 2C) does not correspond to a major interference of the Cstrep tag with the Pol activity at an early stage of the viral cycle, and it contributes to the validation of the MZ-Cstrep-WSN virus as an appropriate tool in the present study. The presence of a One-Strep tag at the N terminus of PB2 had no significant effect on the accumulation of the NP and M1 proteins but led to slightly decreased levels of the PB2 and PB1 proteins in cells infected with P908-Nstrep-WSN as well as MZ-Nstrep-WSN (Fig. 3) (M1 signals were detectable only after a longer exposure time [data not shown]). When the same comparative Western blot analysis was performed for 293T and DF1 cells infected at a high MOI, the results were similar to those ob-

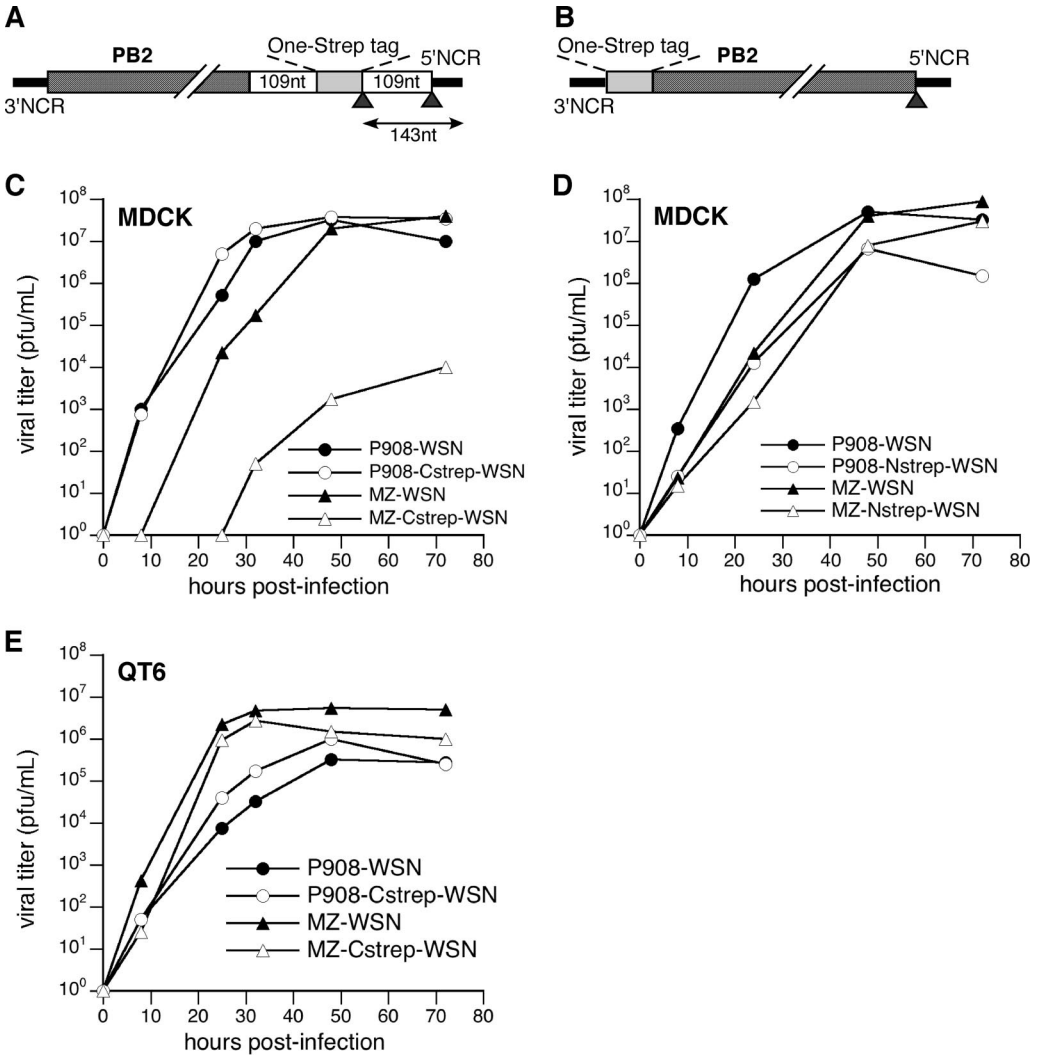

FIG. 2. Characterization of recombinant MZ-WSN and P908-WSN influenza viruses with a PB2 segment encoding a PB2-Strep fusion protein. (A and B) Schematic representation of the PB2 vRNAs expressed in plasmid-based reverse genetics experiments to produce recombinant viruses expressing a PB2 protein fused to the One-Strep tag at the C terminus (A) or at the N terminus (B). The PB2-ORF (hatched box) is fused to the sequence encoding the One-Strep tag (gray box) and flanked by the 3′ and 5′ NCRs (black lines). In panel A the duplicated PB2-ORF sequences are represented as white boxes, and the sequence, which is identical to the wt PB2 vRNA at the 5′ end, is indicated by a double-headed arrow. The stop codons are indicated by black arrowheads. (C to E) Growth curves of the P908-WSN and MZ-WSN viruses compared to the P908-Cstrep-WSN and MZ-Cstrep-WSN viruses on MDCK cells (C) or on QT6 cells (E) and compared to the P908-Nstrep-WSN and MZ-Nstrep-WSN viruses on MDCK cells (D). Cell monolayers were infected at an MOI of 0.001 and incubated for 72 h at 37°C. At the indicated time points, the supernatants were harvested, and virus titers were determined by plaque assays on MDCK cells (for P908-WSN, P908-Cstrep-WSN and P908-Nstrep-WSN) or on QT6 cells (for MZ-WSN, MZ-Cstrep-WSN and MZ-Nstrep-WSN). nt, nucleotides.

tained for MDCK and QT6 cells, respectively (data not shown).

An indirect immunofluorescence assay was used to analyze 293T cells at 2 and 6 h following infection at high MOIs with MZ-WSN or P908-WSN viruses expressing an HA-tagged PB2 protein. Striking differences in the intensity and cellular localization of NP staining were observed. In P908-HA-WSN-infected cells, the NP protein was nuclear at 2 h p.i. (Fig. 4, columns C and D, row a) and mainly cytoplasmic at 6 h p.i. (Fig. 4, columns C and D, row c). In MZ-HA-WSN-infected cells, the NP-specific fluorescence was almost undetectable at 2 h p.i. (Fig. 4, columns C and D, row b) and limited to the nucleus at 6 h p.i. (Fig. 4, columns C and D, row d). At both time points, the PB2-HA protein was detected mainly in the nucleus of infected cells (Fig. 4, columns A and B, rows a to d), and the signal was much stronger in P908-HA-WSN-infected cells (as a consequence, different settings had to be used for P908-HA-WSN and MZ-HA-WSN samples shown in Fig. 4, columns A and B). These observations were in agreement both with the delayed viral multiplication (Fig. 1) and reduced accumulation of PB2 and NP proteins (Fig. 3) observed upon infection of MDCK cells with the MZ-WSN compared to the P908-WSN virus.

We next asked whether the replicative potential of MZ-WSN and P908-WSN viruses could be correlated to the efficiency with which the RNP components interacted with each

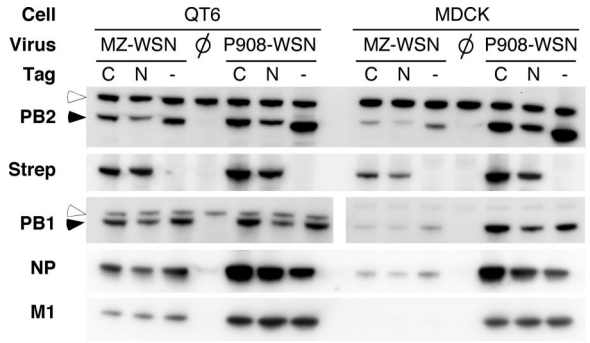

FIG. 3. Western blot analysis of the steady-state levels of viral proteins in cells infected with recombinant MZ-WSN and P908-WSN influenza viruses expressing a PB2-Strep fusion protein. Whole-cell lysates were prepared from MDCK or QT6 cells at 6 h p.i. with the P908-WSN or MZ-WSN viruses expressing either a PB2-wt (−), PB2-Cstrep (C), or PB2-Nstrep (N) protein, as indicated. The samples were loaded on a 4 to 12% polyacrylamide gel and analyzed by Western blotting as described in Materials and Methods, using either a polyclonal antibody directed against the PB2 or PB1 protein, a polyclonal serum recognizing the NP and M1 proteins, or a monoclonal antibody specific for the One-Strep epitope. The positions of the PB2 and PB1 proteins (filled arrowheads) and of cellular proteins recognized nonspecifically by the anti-PB2 and anti-PB1 antibodies (open arrowheads) are indicated.

other and with cellular partners, by performing copurification experiments on cells infected with the corresponding PB2-Strep viruses. Because reagents are more readily available for human and chicken cellular proteins, these experiments were set up on 293T and DF1 cells.

Copurification of viral core proteins from human or avian cells infected with PB2-Strep viruses. We first compared how efficiently the P908 and MZ viral Pols assembled and interacted with the NP in 293T and DF1 cells. Confluent cell monolayers were infected at a high MOI with the P908- or MZ-Cstrep-WSN viruses in parallel with the control P908- or MZ-WSN viruses and incubated at 37°C or 33°C. Total cell extracts were prepared at 6 h p.i. as described in the Materials and Methods section and were incubated with Strep-tactin beads. After the beads were washed, PB2-Strep complexes were eluted using Laemmli buffer, separated by electrophoresis on a denaturing gel, and analyzed by Western blotting using antibodies specific for the viral PB2, PB1, PA, and NP proteins.

For each of the Pol subunits, protein levels upon infection with the MZ-Cstrep-WSN or P908-Cstrep-WSN virus were compared in total lysates prepared from infected 293T or DF1 cells and in the corresponding Strep-tactin eluates. For the

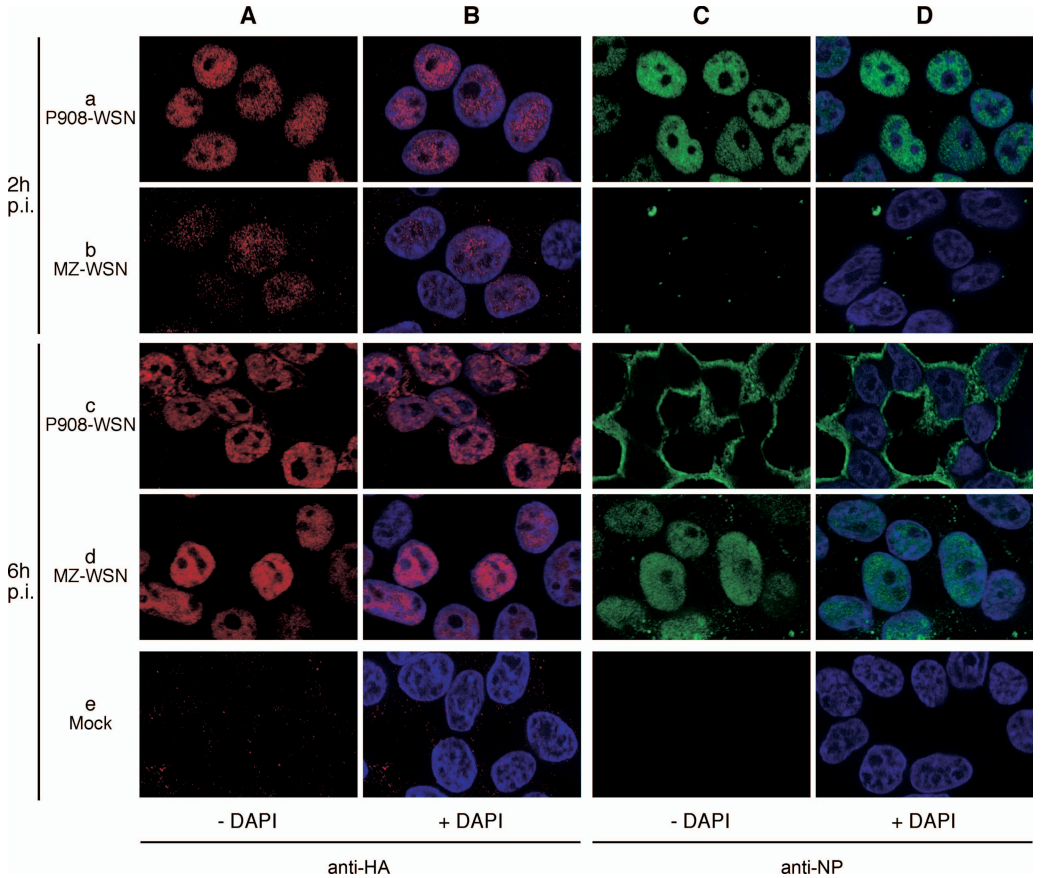

FIG. 4. Intracellular distribution of PB2 and NP in 293T cells infected with a P908-WSN or MZ-WSN virus expressing a PB2-HA fusion protein. 293T cells were infected at an MOI of 2 with the P908-HA-WSN or MZ-HA-WSN virus expressing a PB2-HA fusion protein and incubated at 37°C. At 2 and 6 h p.i., immunofluorescence assays were performed as described in Materials and Methods, using either an anti-HA (red staining) or an anti-NP (green staining) monoclonal antibody. In columns A and B, distinct settings had to be used because of the low signal levels in MZ-WSN samples. The same settings were used for all data shown in columns C and D. Columns B and D represent merges between the anti-HA or anti-NP stainings shown in columns A and C, respectively, and the DAPI (4′,6′-diamidino-2-phenylindole) nucleic acid staining of the same fields (blue staining).

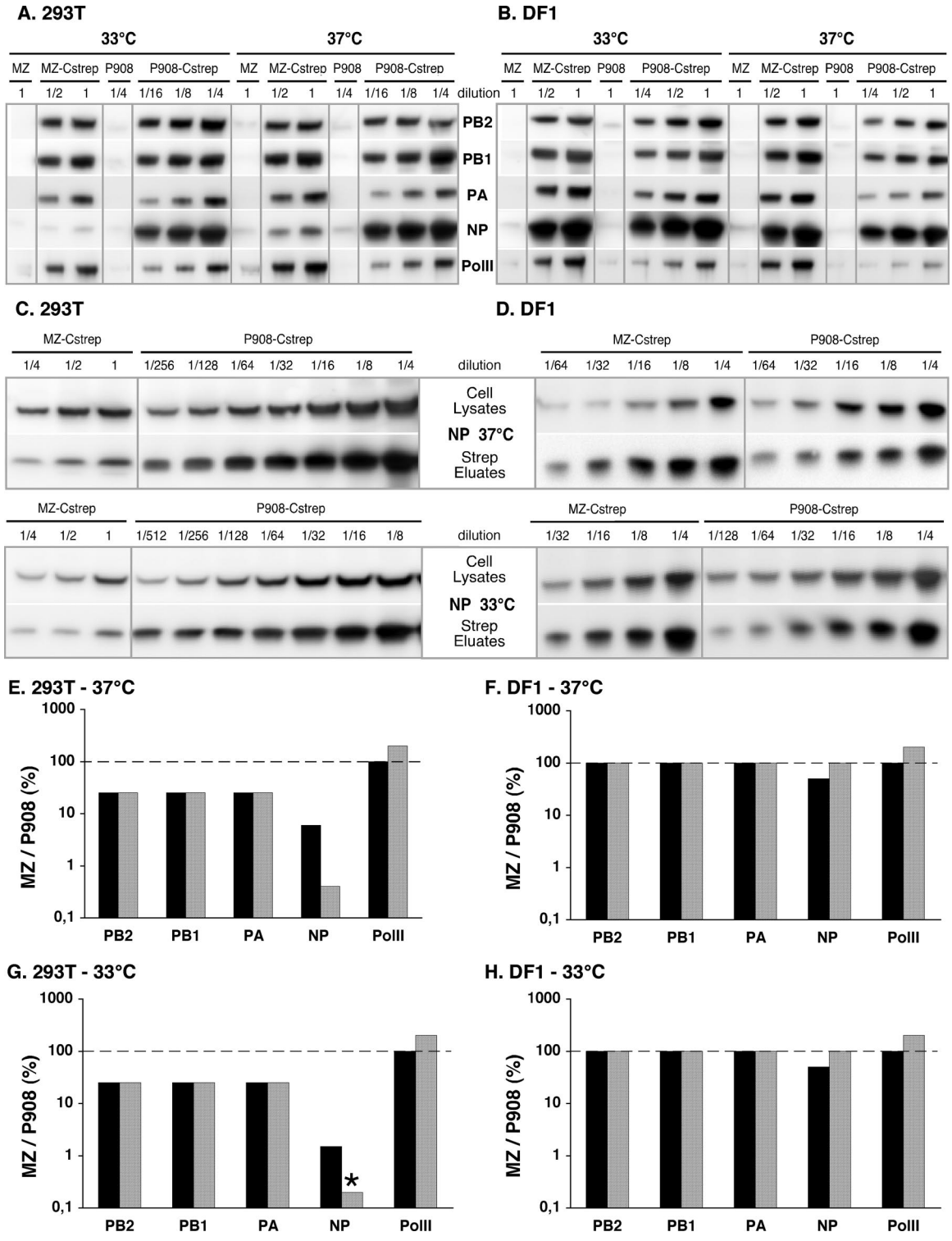

FIG. 5. Western blot analysis of P908-Cstrep-WSN- or MZ-Cstrep-WSN-infected cell lysates before and after purification on Strep-tactin beads. (A and B) Analysis of protein complexes eluted from Strep-tactin beads. 293T or DF1 cells were infected at an MOI of 2 with MZ-WSN (MZ), MZ-Cstrep-WSN (MZ-Cstrep), P908-WSN (P908), or P908-Cstrep-WSN (P908-Cstrep) virus and incubated at 37 or 33°C for 6 h. Whole-cell lysates were prepared, and a fraction was incubated with Strep-tactin beads as described in Materials and Methods. Protein complexes were eluted and serially diluted in Laemmli buffer, loaded on a 4 to 12% sodium dodecyl sulfate-polyacrylamide gel, and analyzed by Western blotting as described in Materials and Methods, using either polyclonal antibodies directed against the PB2, PB1, PA, or NP protein or a monoclonal antibody specific for the cellular RNA Pol II, as indicated. (C and D) Analysis of the levels of NP protein before and after purification on Strep-tactin beads. The whole-cell lysates and the Strep-tactin eluates prepared from infected 293T or DF1 cells were serially diluted in whole-cell lysates prepared from uninfected cells and in Laemmli buffer, respectively, loaded on a 4 to 12% sodium dodecyl sulfate-polyacrylamide gel, and analyzed by Western blotting, as described in Materials and Methods, using a polyclonal antibody recognizing the NP protein. The samples

purpose of quantification, serial dilutions of the pre- and post-purification samples were analyzed using the G-Box and GeneTools software (Syngene). Very reproducible results were obtained in three independent experiments. Similar observations were made at 37°C and 33°C. In total cell lysates, for each of the Pol subunits, the signal ratios of MZ-Cstrep-WSN to P908-Cstrep-WSN were about 1:4 to 1:8 in 293T cells (Fig. 5E and G) and 1:1 in DF1 cells (Fig. 5F and H). In Strep-tactin eluates derived from 293T infected cell extracts, the protein ratios of MZ-Cstrep-WSN to P908-Cstrep-WSN were still about 1:4 to 1:8 for PB2-Strep as well as for the PB1 and PA subunits (Fig. 5A, E, and G). That the ratios before and after purification for all three subunits were the same suggests that assembly of the MZ Pol complex is not impaired in 293T cells although each subunit is underexpressed. Similarly, the 1:1 protein ratios of MZ to P908 in DF1 samples was conserved throughout the purification process (Fig. 5B, F, and H), suggesting that both viral Pols are being assembled with the same efficiency in avian cells.

Analysis of the levels of NP protein upon infection with MZ- and P908-Cstrep-WSN viruses also showed marked differences in 293T but not in DF1 cells. In DF1 cell lysates analyzed prior to purification, similar NP signals were detected whether the cells had been infected with the MZ- or the P908-Cstrep-WSN virus (Fig. 5D, cell lysates, F, and H). Subsequently, similar levels of MZ- and P908-NP appeared to copurify with MZ- and P908-PB2-Cstrep, respectively (Fig. 5D, eluates, F, and H). In contrast, 293T cells infected with the MZ-Cstrep-WSN virus showed significantly reduced NP levels compared to P908-Cstrep-WSN-infected cells. The difference was about 16- to 32-fold when cells had been incubated at 37°C and 64- to 128-fold when cells were incubated at 33°C (Fig. 5C, lysates, E, and G). The relatively high levels of NP in P908-Cstrep-WSN-infected cells (Fig. 3 and related comments) accounted in part for the broad difference. When this corrective factor was taken into account, the reduction of MZ-NP levels was still repeatedly more pronounced than the reduction of MZ-Pol levels in 293T cells incubated at 33°C. After Strep-tactin purification, the estimated ratios of MZ-NP to P908-NP were about 1:256 and <1:512 when 293T cells were incubated at 37 and 33°C, respectively (Fig. 5C, eluates, E, and G). These lower ratios compared to those observed in total cell extracts (about 1:32 and 1:128 at 37 and 33°C, respectively, as mentioned above) raised the possibility of a specific defect of the association between the MZ-NP and MZ-Pol in 293T cells. Whether this defect was more pronounced at 33°C than at 37°C could not be established because of weak MZ-NP signals in 293T cells infected at 33°C (Fig. 5G).

Copurification experiments were repeated using the MZ- and P908-WSN viruses tagged at the N terminus instead of the C terminus of PB2. When protein ratios were compared in Strep-tactin eluates (Fig. 6) and in total cell extracts (Fig. 6), the ratios of MZ-PB2 to P908-PB2 and of MZ-PB1 to P908-PB1 appeared essentially unchanged. In contrast, the ratio of MZ-NP to P908-NP was decreased at least twofold in Strep-tactin eluates compared to total cell extracts. The extent to which the NP ratio was decreased could not be evaluated precisely because the signals corresponding to MZ-NP were at background levels (Fig. 6). The overall signal intensity in experiments with Nstrep viruses was low compared to Cstrep viruses due to low levels of expression (Fig. 3) and purification yield (data not shown) of PB2-Nstrep compared to PB2-Cstrep proteins. However, the data obtained with Nstrep viruses indicated a defect of the association between MZ-NP and MZ-Pol in 293T cells and were in agreement with those obtained with Cstrep viruses.

The impact of a Glu-to-Lys substitution at residue 627 of MZ-PB2 on the efficiency of copurification of the viral core proteins was finally examined. Avian-like MZ-WSN and MZ-Cstrep-WSN viruses with a PB2-627 Glu-to-Lys substitution (627K) were produced. A copurification experiment was per-

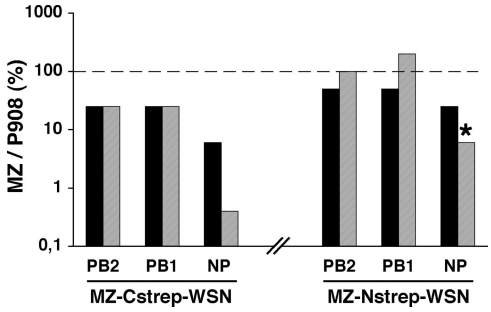

FIG. 6. Western blot analysis of P908-Nstrep-WSN- or MZ-Nstrep-WSN-infected cell lysates before and after purification on Strep-tactin beads. 293T cells were infected at an MOI of 2 with MZ-WSN, MZ-Cstrep-WSN, P908-WSN, or P908-Cstrep-WSN virus in one experiment and with MZ-WSN, MZ-Nstrep-WSN, P908-WSN, or P908-Nstrep-WSN virus in an independent experiment and incubated at 37°C for 6 h. Whole-cell lysates were prepared, a fraction was incubated with Strep-tactin beads, and eluted protein complexes were analyzed using polyclonal antibodies directed against the PB2, PB1, or NP protein, as described in the legend of Fig. 5. The signals measured in samples derived from MZ-Cstrep-WSN- and MZ-Nstrep-WSN-infected cells were compared to those measured in samples derived from P908-Cstrep-WSN- and P908-Nstrep-WSN-infected cells, respectively, taking into account the sample dilution factor. The MZ/P908 ratios measured in total cell extracts (black bars) and in Strep-tactin eluates (gray bars) are expressed as percentages. The percentage indicated by the asterisk is overestimated because the MZ-NP signal was at background levels. The results of one representative experiment out of three (Cstrep viruses) or out of two (Nstrep viruses) are shown.

are from the same experiment as shown in panels A and B, respectively. The sample dilution factors are indicated using the following notation: 1, undiluted; 1/2, diluted twofold, 1/4, diluted fourfold, and so on. (E to H) Graphic representation of the results of Western blot quantification. After the membranes were scanned using a G-Box (SynGene), the signals corresponding to the PB2, PB1, PA, NP, or RNA Pol II proteins were quantified using the GeneTools software (SynGene). The signals measured in samples derived from MZ-Cstrep-WSN-infected cells were compared to those measured in samples derived from P908-Cstrep-WSN-infected cells, taking into account the sample dilution factor. The MZ/P908 ratios measured in total cell extracts (black bars) and in Strep-tactin eluates (gray bars) are expressed as percentages. The percentage indicated by the asterisk is overestimated due to the fact that the MZ-NP signal was at background levels. The results of one representative experiment out of three are shown.

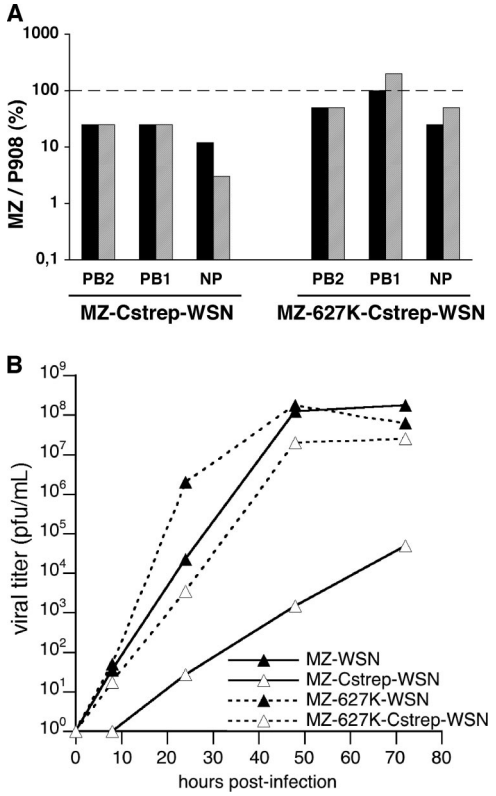

FIG. 7. Effect of the Glu-Lys substitution at PB2 residue 627 on the phenotype of the avian-like MZ-WSN viruses. (A) Western blot analysis of mutant or wt MZ-Cstrep-WSN-infected cell lysates before and after purification on Strep-tactin beads. 293T cells were infected at an MOI of 2 with the P908-WSN, MZ-WSN, MZ-627K-WSN, P908-Cstrep-WSN, MZ-Cstrep-WSN, or MZ-627K-Cstrep-WSN virus and incubated at 37°C for 6 h. Whole-cell lysates were prepared, a fraction was incubated with Strep-tactin beads, and eluted protein complexes were analyzed using polyclonal antibodies directed against the PB2, PB1, or NP protein, as described in the legend to Fig. 5. The signals measured in samples derived from MZ-Cstrep-WSN- and MZ-627K-Cstrep-WSN-infected cells were compared to those measured in samples derived from P908-Cstrep-WSN-infected cells, taking into account the sample dilution factor. The MZ/P908 ratios measured in total cell extracts (black bars) and in Strep-tactin eluates (gray bars) are expressed as percentages. (B) Growth curves of the 627K mutant compared to the wt MZ-WSN and MZ-Cstrep-WSN viruses on MDCK cells. Cell monolayers were infected at an MOI of 0.001 and incubated for 72 h at 37°C. At the indicated time points, the supernatants were harvested, and virus titers were determined by plaque assays on QT6 cells.

formed on cell extracts prepared from 293T cells infected at a high MOI with the MZ-627K-Cstrep-WSN, MZ-Cstrep-WSN, or P908-Cstrep-WSN virus in parallel with the control MZ-627K-WSN, MZ-WSN, or P908-WSN virus. No reduction of the ratio of MZ-NP to P908-NP in Strep-tactin eluates compared to total cell extracts was observed upon infection with the MZ-627K-Cstrep-WSN virus, unlike with the MZ-Cstrep-WSN virus (a fourfold reduction) (Fig. 7A). This observation indicated that the presence of a Lys instead of a Glu at PB2 residue 627 fully corrected the defect of NP association with the Pol in MZ-Cstrep-WSN-infected cells. Following infection of MDCK cells at a low MOI (0.001), the mutant MZ-627K-WSN and MZ-627K-Cstrep-WSN viruses grew more efficiently than their wt counterparts (Fig. 7B). Notably, the mutant MZ-627K-Cstrep-WSN still showed delayed growth kinetics compared to the untagged mutant MZ-627K-WSN virus, which strongly suggests that the growth defect due to the presence of the Cstrep tag was not corrected by the Glu627Lys substitution and, thus, was unrelated to the defect of NP-Pol association.

Copurification of viral Pol and cellular RNA Pol II from human or avian cells infected with PB2-Cstrep viruses. Engelhardt et al. showed the existence of a physical association between the influenza WSN virus Pol and the large subunit of the cellular RNA Pol II in a transcriptionally active, hyperphosphorylated form (7). Here, we compared how efficiently the P908 and MZ viral Pols interacted with the Pol II enzyme in 293T and DF1 cells. Total cell lysates were analyzed by Western blotting using the monoclonal antibody 8WG16, which allows detection of two forms of the Pol II large subunit C-terminal domain corresponding to different phosphorylation states of the protein (7). In 293T as well as in DF1 cells, both forms of Pol II were detected at similar levels whether the cells had been mock infected or infected with the MZ-Cstrep-WSN or the P908-Cstrep-WSN virus (data not shown). Following purification on Strep-tactin beads, some Pol II was detected specifically in the samples corresponding to cells infected with PB2-Cstrep viruses (Fig. 5A and B), and this protein was found to correspond to the slow mobility form (data not shown). Comparison of the signal ratios of PB2/PB1/PA to Pol II indicated that the human Pol II enzyme (Fig. 5A, E, and G) as well as the chicken Pol II enzyme (Fig. 5B, F, and H) copurified more efficiently with the MZ Pol than with the P908 Pol. Depending on the experiments, the ratio of Pol II to PB1 was two- to eightfold higher in cells infected with MZ-Cstrep-WSN than with P908-Cstrep-WSN. Overall, these observations clearly indicated that the replication defect of the MZ virus in 293T cells was not related to an impaired binding of the Pol complex to the cellular Pol II.

DISCUSSION

In the present study, the growth properties of recombinant influenza viruses expressing the core proteins from a human (P908) or an avian (MZ) isolate in the background of the WSN strain were compared. Both reassortant viruses replicated efficiently on avian cultured cells, as did both parental isolates. This argues against any major incompatibility between the core proteins derived from the isolates and the viral proteins derived from WSN virus. On mammalian cells, the avian parental isolate and the corresponding reassortant showed restricted growth, compared to their human counterpart, at 37°C and even more so at lower temperatures. Thus, growth restriction and cold sensitivity of the avian isolate on mammalian cultured cells were largely determined by the RNP genes, in agreement with previous data showing reduced transcription/replication activities of RNPs derived from avian compared to human influenza A viruses upon reconstitution in mammalian cells (16, 20).

We successfully generated recombinant P908-WSN and MZ-WSN viruses expressing a PB2 protein fused to a One-Strep or an HA tag at the C terminus by using a procedure described previously: the 109 last nucleotides encoding PB2 were duplicated downstream of the tag sequence so that the

PB2 genomic segment retained the packaging signals present at its 5′ end (4). Recombinant viruses expressing a PB2 protein fused to a One-Strep tag at the N terminus were also successfully produced and did not require any duplication of viral sequences. The recombinant P908-WSN and MZ-WSN viruses expressing a tagged PB2 protein grew to high titers and remained genetically stable upon amplification on MDCK and DF1 cells, respectively. Thus, the procedure we described initially for the production of recombinant WSN viruses expressing a PB2-Flag or a Flag-PB2 protein (4) is applicable to other viruses with PB2 segments of different origins, and tags of various lengths and sequences can be accommodated. The same procedure might be used to generate recombinant viruses expressing a tagged PB1 or PA protein as the sequences required for effective incorporation of the corresponding vRNA into virions have now been mapped on both the 3′ and 5′ ends (17, 19).

The One-Strep tag has been described as an efficient tool to purify protein complexes from crude extracts under mild elution conditions and with good yields (18). Indeed, the PB2-Strep viruses allowed us to compare the efficiency with which the components from the P908- and MZ-derived RNPs interacted with each other and with cellular partners in human and in avian cells infected at high MOIs. In avian DF1 cells, the core proteins were expressed at similar levels whether the cells had been infected with MZ-Cstrep-WSN or P908-Cstrep-WSN. Both the avian- and human-derived Pol complexes were efficiently assembled and bound to the NP protein. In 293T cells, the PB1, PB2, and PA proteins were underexpressed when the cells had been infected with MZ-Cstrep-WSN compared to P908-Cstrep-WSN, in agreement with the low transcription/replication activity of MZ-RNPs in 293T cells described previously (16). However, similar ratios of MZ-PB1 to P908-PB1 and of MZ-PA to P908-PA in total cell lysates and in Strep-tactin eluates, at 37°C as well as at 33°C, indicated that the assembly of the avian-derived Pol complex was not impaired in 293T cells. Experiments using the set of viruses with a One-Strep tag at the N terminus instead of the C terminus of PB2 led to similar findings. According to a recently proposed model, PB1 and PA are imported into the nucleus as a PB1-PA dimer associated with RanBP5, which then dissociates from RanBP5 and assembles with separately imported PB2 (2). The D701N mutation in PB2 was found both to mediate adaptation of the avian influenza virus SC35 to mice (10) and to increase binding of PB2 to importin α1 in 293T cells (11), suggesting that molecular interactions between the Pol and the nuclear import machinery might play a role in host adaptation. However, our copurification data, taken together with the fact that immunofluorescence analysis revealed no cytoplasmic accumulation of the MZ-PB2 protein in 293T infected cells, suggest that a defect in nuclear import of PB2 or in assembly of the Pol complex is not the major mechanism underlying growth restriction of the avian MZ-WSN virus in 293T cells.

As observed for the Pol subunits, the NP protein accumulated at lower levels in 293T cells infected with MZ-Cstrep-WSN than with P908-Cstrep-WSN. The difference was more pronounced for the NP protein than for the Pol subunits and markedly so when 293T cells were incubated at 33°C. One hypothesis is that the half-life of the MZ-derived NP protein might be specifically reduced in human cells by a temperature-dependent mechanism. It has been suggested that BAT1 and Tat-SF1 may function as molecular chaperones for NP and facilitate NP-vRNA interaction (24, 26). Poor recognition of MZ-NP by the human BAT1 or Tat-SF1 factor might result in NP aggregation and/or an increased degradation rate. Using an anti-NP antibody for immunofluorescence assays, we observed a pattern of punctuated cytoplasmic dots in 293T cells infected with the MZ-WSN virus, which was not visible in 293T cells infected with the P908-WSN virus and which could correspond to NP aggregates (Fig. 4, columns C and D). A defect of association with the Pol could also contribute to a decreased half-life of the MZ-NP protein. Indeed, our results point to inefficient NP-Pol association as a characteristic that differentiates MZ from P908 upon infection in 293T cells. The amounts of NP copurifying with the Pol complex were about 8- to 16-fold lower than expected based on the overall reduced levels of NP in 293T cells infected with the MZ-Cstrep-WSN compared to the P908-Cstrep-WSN virus. When Western blot analysis was performed under nondenaturing conditions, high-molecular-weight complexes, most likely including viral Pol and multimeric NP, were detected in cells infected with P908-Cstrep-WSN but not with MZ-Cstrep-WSN (data not shown). A similar defect of association of MZ-NP with the Pol was observed in experiments using the MZ- and P908-Nstrep-WSN viruses. A Glu-to-Lys substitution at residue 627 of MZ-PB2 resulted in increased levels of expression of the MZ core proteins in 293T cells and efficient association of MZ-NP with the Pol complex. Our findings suggest that residue 627 of PB2 modulates the efficiency of NP binding to the Pol in human cells during the course of infection, in agreement with data obtained upon transient expression of the viral core proteins in 293T cells by us (16) and by others (23).

A concern was that the results obtained with the MZ-Cstrep-WSN viruses could correspond to artifacts due to the presence of the tag, as this virus showed reduced growth on MDCK cells compared to its untagged MZ-WSN counterpart in a multicycle growth assay. However, a defect of the association between MZ-NP and MZ-Pol in 293T cells was observed with the Nstrep viruses, which did not exhibit a growth defect, as well as with the Cstrep viruses. In addition, our data on MZ-WSN viruses with a Glu-to-Lys substitution at residue 627 strongly suggested that the growth defect due to the presence of the Cstrep tag was not related to the defect of the NP-Pol association as it was not corrected by the presence of a Lys627. Finally, the fact that the PB1, PB2, NP, and M1 proteins, as well as the M vRNAs (as evaluated by quantitative RT-PCR at 6 h p.i.) (data not shown) were detected at similar levels in MDCK cells infected with the MZ-Cstrep-WSN and MZ-WSN viruses also indicates the absence of a major perturbation of the Pol activity due to the One-Strep tag, at least at early stages of the viral cycle, and contributes to validate the MZ-Cstrep-WSN virus as an appropriate tool in our study.

In DF1 cells unlike in 293T cells, NP binding to the Pol was equally efficient for MZ and P908, suggesting that cellular factor(s) are likely involved in the control of the NP-Pol interaction. This hypothesis is consistent with the three-dimensional structure of the PB2-627 domain recently reported by Tarendeau et al. (36). Residue 627 is present at the surface of the domain and could well be involved in molecular interactions with viral and/or cellular proteins. We believe that comparative

proteomic analyses using the recombinant P908-Cstrep-WSN and MZ-Cstrep-WSN viruses is a powerful approach to identify such cellular factor(s) and to understand their role in controlling the host range of influenza viruses. As a proof of concept, we were able in the present study to demonstrate that the Pol of the avian MZ virus interacts with the human RNA Pol II more strongly than does the Pol of the human P908 virus in 293T infected cells and also does so with the chicken RNA Pol II enzyme in DF1 infected cells. Our work extends the initial observation by Engelhardt et al. that the Pol of the WSN strain interacts with the human RNA Pol II (7) and reinforces their suggestion that this interaction plays a key role in the viral cycle. Furthermore, our data indicate that growth restriction of avian influenza viruses in human cells is not related to a defect in the physical association between the viral Pol and cellular Pol II. It still remains possible that this association is taking place in such a way that the corresponding function is not preserved. A precise investigation of the spatial and temporal distribution of viral RNPs in the course of infection, using recombinant viruses expressing a tagged Pol, should help improve our understanding of the functional interactions between RNPs and host factors.

ACKNOWLEDGMENTS

We are grateful to G. Brownlee for providing the plasmids for reverse genetics of the WSN strain; to J. Ortin (Centro Nacional de Biotecnologia, Madrid, Spain) for providing polyclonal antibodies specific for PB1, PB2, and PA; and to J. Pavlovic (Institut für Medizinishe Virologie, Zurich, Switzerland) for providing the pHMG plasmid. The technical assistance of Monica Marasescu and Sébastien Le Gal is gratefully acknowledged.

M.-A.R.-W. was supported by a fellowship from the Institut Pasteur. A.T. was supported by a fellowship from the Region Ile-de-France. This work was supported in part by the FLUINNATE (SP5B-CT-2006-044161) program.

REFERENCES

1. **Crescenzo-Chaigne, B., N. Naffakh, and S. van der Werf.** 1999. Comparative analysis of the ability of the polymerase complexes of influenza viruses type A, B and C to assemble into functional RNPs that allow expression and replication of heterotypic model RNA templates in vivo. Virology **265:**342–353.
2. **Deng, T., O. G. Engelhardt, B. Thomas, A. V. Akoulitchev, G. G. Brownlee, and E. Fodor.** 2006. Role of ran binding protein 5 in nuclear import and assembly of the influenza virus RNA polymerase complex. J. Virol. **80:** 11911–11919.
3. **Digard, P., D. Elton, K. Bishop, E. Medcalf, A. Weeds, and B. Pope.** 1999. Modulation of nuclear localization of the influenza virus nucleoprotein through interaction with actin filaments. J. Virol. **73:**2222–2231.
4. **Dos Santos Afonso, E., N. Escriou, I. Leclercq, S. van der Werf, and N. Naffakh.** 2005. The generation of recombinant influenza A viruses expressing a PB2 fusion protein requires the conservation of a packaging signal overlapping the coding and noncoding regions at the 5′ end of the PB2 segment. Virology **341:**34–46.
5. **Elton, D., M. Simpson-Holley, K. Archer, L. Medcalf, R. Hallam, J. McCauley, and P. Digard.** 2001. Interaction of the influenza virus nucleoprotein with the cellular CRM1-mediated nuclear export pathway. J. Virol. **75:**408–419.
6. **Engelhardt, O. G., and E. Fodor.** 2006. Functional association between viral and cellular transcription during influenza virus infection. Rev. Med. Virol. **16:**329–345.
7. **Engelhardt, O. G., M. Smith, and E. Fodor.** 2005. Association of the influenza A virus RNA-dependent RNA polymerase with cellular RNA polymerase II. J. Virol. **79:**5812–5818.
8. **Fodor, E., L. Devenish, O. G. Engelhardt, P. Palese, G. G. Brownlee, and A. Garcia-Sastre.** 1999. Rescue of influenza A virus from recombinant DNA. J. Virol. **73:**9679–9682.
9. **Gabriel, G., M. Abram, B. Keiner, R. Wagner, H. D. Klenk, and J. Stech.** 2007. Differential polymerase activity in avian and mammalian cells determines host range of influenza virus. J. Virol. **81:**9601–9604.
10. **Gabriel, G., B. Dauber, T. Wolff, O. Planz, H. D. Klenk, and J. Stech.** 2005. The viral polymerase mediates adaptation of an avian influenza virus to a mammalian host. Proc. Natl. Acad. Sci. USA **102:**18590–18595.
11. **Gabriel, G., A. Herwig, and H. D. Klenk.** 2008. Interaction of polymerase subunit PB2 and NP with importin α1 is a determinant of host range of influenza A virus. PLoS Pathog. **4:**e11.
12. **Hirayama, E., H. Atagi, A. Hiraki, and J. Kim.** 2004. Heat shock protein 70 is related to thermal inhibition of nuclear export of the influenza virus ribonucleoprotein complex. J. Virol. **78:**1263–1270.
13. **Huarte, M., J. J. Sanz-Ezquerro, F. Roncal, J. Ortin, and A. Nieto.** 2001. PA subunit from influenza virus polymerase complex interacts with a cellular protein with homology to a family of transcriptional activators. J. Virol. **75:**8597–8604 .
14. **Jorba, N., S. Juarez, E. Torreira, P. Gastaminza, N. Zamarreno, J. P. Albar, and J. Ortin.** 2008. Analysis of the interaction of influenza virus polymerase complex with human cell factors. Proteomics **8:**2077–2088.
15. **Kawaguchi, A., and K. Nagata.** 2007. De novo replication of the influenza virus RNA genome is regulated by DNA replicative helicase, MCM. EMBO J. **26:**4566–4575.
16. **Labadie, K., E. Dos Santos Afonso, M. A. Rameix-Welti, S. van der Werf, and N. Naffakh.** 2007. Host-range determinants on the PB2 protein of influenza A viruses control the interaction between the viral polymerase and nucleoprotein in human cells. Virology **362:**271–282.
17. **Liang, Y., T. Huang, H. Ly, T. G. Parslow, and Y. Liang.** 2008. Mutational analyses of packaging signals in influenza virus PA, PB1, and PB2 genomic RNA segments. J. Virol. **82:**229–236.
18. **Lichty, J. J., J. L. Malecki, H. D. Agnew, D. J. Michelson-Horowitz, and S. Tan.** 2005. Comparison of affinity tags for protein purification. Protein Expr. Purif. **41:**98–105.
19. **Marsh, G. A., R. Rabadan, A. J. Levine, and P. Palese.** 2008. Highly conserved regions of influenza a virus polymerase gene segments are critical for efficient viral RNA packaging. J. Virol. **82:**2295–2304.
20. **Massin, P., S. van der Werf, and N. Naffakh.** 2001. Residue 627 of PB2 is a determinant of cold sensitivity in RNA replication of avian influenza viruses. J. Virol. **75:**5398–5404.
21. **Matrosovich, M., T. Matrosovich, W. Garten, and H. D. Klenk.** 2006. New low-viscosity overlay medium for viral plaque assays. Virol. J. **3:**63.
22. **Mayer, D., K. Molawi, L. Martinez-Sobrido, A. Ghanem, S. Thomas, S. Baginsky, J. Grossmann, A. Garcia-Sastre, and M. Schwemmle.** 2007. Identification of cellular interaction partners of the influenza virus ribonucleoprotein complex and polymerase complex using proteomic-based approaches. J. Proteome Res. **6:**672–682.
23. **Mehle, A., and J. A. Doudna.** 2008. An inhibitory activity in human cells restricts the function of an avian-like influenza virus polymerase. Cell Host Microbe **4:**111–122.
24. **Momose, F., C. F. Basler, R. E. O'Neill, A. Iwamatsu, P. Palese, and K. Nagata.** 2001. Cellular splicing factor RAF-2p48/NPI-5/BAT1/UAP56 interacts with the influenza virus nucleoprotein and enhances viral RNA synthesis. J. Virol. **75:**1899–1908.
25. **Naffakh, N., A. Tomoiu, M. A. Rameix-Welti, and S. van der Werf.** 2008. Host-restriction of avian influenza viruses at the level of the ribonucleoproteins. Ann. Rev. Microbiol. **62:**403–424.
26. **Naito, T., Y. Kiyasu, K. Sugiyama, A. Kimura, R. Nakano, A. Matsukage, and K. Nagata.** 2007. An influenza virus replicon system in yeast identified Tat-SF1 as a stimulatory host factor for viral RNA synthesis. Proc. Natl. Acad. Sci. USA **104:**18235–18240.
27. **Naito, T., F. Momose, A. Kawaguchi, and K. Nagata.** 2007. Involvement of Hsp90 in assembly and nuclear import of influenza virus RNA polymerase subunits. J. Virol. **81:**1339–1349.
28. **Neumann, G., G. G. Brownlee, E. Fodor, and Y. Kawaoka.** 2004. Orthomyxovirus replication, transcription, and polyadenylation. Curr. Top. Microbiol. Immunol. **283:**121–143.
29. **Neumann, G., and Y. Kawaoka.** 2006. Host range restriction and pathogenicity in the context of influenza pandemic. Emerg. Infect. Dis. **12:**881–886.
30. **Rogers, G. N., and J. C. Paulson.** 1983. Receptor determinants of human and animal influenza virus isolates: differences in receptor specificity of the H3 hemagglutinin based on species of origin. Virology **127:**361–373.
31. **Salomon, R., J. Franks, E. A. Govorkova, N. A. Ilyushina, H. L. Yen, D. J. Hulse-Post, J. Humberd, M. Trichet, J. E. Rehg, R. J. Webby, R. G. Webster, and E. Hoffmann.** 2006. The polymerase complex genes contribute to the high virulence of the human H5N1 influenza virus isolate A/Vietnam/1203/04. J. Exp. Med. **203:**689–697.
32. **Schmidt, G. M., and A. Skerra.** 2007. The Strep-tag system for one-step purification and high-affinity detection or capturing of proteins. Nat. Protoc. **2:**1528–1535.
33. **Shinya, K., S. Watanabe, T. Ito, N. Kasai, and Y. Kawaoka.** 2007. Adaptation of an H7N7 equine influenza A virus in mice. J. Gen. Virol. **88:**547–553.
34. **Suzuki, Y., T. Ito, T. Suzuki, R. E. Holland, Jr., T. M. Chambers, M. Kiso, H. Ishida, and Y. Kawaoka.** 2000. Sialic acid species as a determinant of the host range of influenza A viruses. J. Virol. **74:**11825–11831.
35. **Tarendeau, F., J. Boudet, D. Guilligay, P. J. Mas, C. M. Bougault, S. Boulo, F. Baudin, R. W. Ruigrok, N. Daigle, J. Ellenberg, S. Cusack, J. P. Simorre,**

and D. J. Hart. 2007. Structure and nuclear import function of the C-terminal domain of influenza virus polymerase PB2 subunit. Nat. Struct. Mol. Biol. **14:**229–233.
36. **Tarendeau, F., T. Crepin, D. Guilligay, R. W. Ruigrok, S. Cusack, and D. J. Hart.** 2008. Host determinant residue lysine 627 lies on the surface of a discrete, folded domain of influenza virus polymerase PB2 subunit. PLoS Pathog. **4:**e1000136.
37. **Vignuzzi, M., S. Gerbaud, S. van der Werf, and N. Escriou.** 2001. Naked RNA immunization with replicons derived from poliovirus and Semliki Forest virus genomes for the generation of a cytotoxic T cell response against the influenza A virus nucleoprotein. J. Gen. Virol. **82:**1737–1747.
38. **Webster, R. G., W. J. Bean, O. T. Gorman, T. M. Chambers, and Y. Kawaoka.** 1992. Evolution and ecology of influenza A viruses. Microbiol. Rev. **56:**152–179.